

MIT Open Access Articles

An offset-cancelling four-phase voltage sense amplifier for resistive memories in 14nm CMOS

The MIT Faculty has made this article openly available. **Please share** how this access benefits you. Your story matters.

Citation: Biswas, Avishek et al. "An offset-cancelling four-phase voltage sense amplifier for resistive memories in 14nm CMOS." IEEE Custom Integrated Circuits Conference (CICC), April-May 2017, Austin, Texas, USA, IEEE Custom Integrated Circuits Conference (CICC), July 2017. © 2017 IEEE

As Published: <http://dx.doi.org/10.1109/cicc.2017.7993689>

Publisher: Institute of Electrical and Electronics Engineers (IEEE)

Persistent URL: <https://hdl.handle.net/1721.1/122465>

Version: Author's final manuscript: final author's manuscript post peer review, without publisher's formatting or copy editing

Terms of use: Creative Commons Attribution-Noncommercial-Share Alike



An Offset-Cancelling Four-Phase Voltage Sense Amplifier for Resistive Memories in 14nm CMOS

Avishek Biswas*, Umut Arslan†, Fatih Hamzaoglu† and Anantha P. Chandrakasan*

*Department of Electrical Engineering and Computer Science,
Massachusetts Institute of Technology, Cambridge, MA 02139, U.S.A
Email: avibiws@mit.edu, anantha@mit.edu

†Intel Corporation, Hillsboro, OR 97124, U.S.A. Email: {umut.arslan, fatih.hamzaoglu}@intel.com

Abstract—This paper presents a low-offset read sensing scheme for resistive memories. Due to increasing device variations in sub-32 nm CMOS processes, it becomes very challenging to design a high yield and low-offset read-sensing scheme. In this work we address these issues by using a pseudo-differential sensing scheme to get $2\times$ signal margin and by full offset cancellation of the sense-amplifier, making it more suitable to tolerate variation from the memory array due to storage device resistance variation. Measurement results show the sense-amplifier can work with a 20mV input, which makes it ideal for small-signal sensing for resistive memories.

I. INTRODUCTION

Resistive memories [1], [2] are a class of non-volatile embedded memories that have the potential to be a universal memory technology by providing the density of DRAM, the speed of SRAM and the non-volatility of Flash. Resistive memories typically consist of a 1T-1R structure [3], [4], with a resistive storage device (e.g. a magnetic tunnel junction or MTJ for Spin-Transfer Torque Random Access Memory (STT-RAM)) and an access transistor. There are two resistance states: high-resistance (R_H ‘1’) and low-resistance (R_L ‘0’), where $R_H = (1 + TMR) \times R_L$. For MTJ devices the tunnel-magneto-resistance ratio (TMR) is typically around 100%-200%, depending on technology, temperature etc., which makes it challenging to distinguish the two resistance states correctly. Also, when a current is passed through an MTJ device to read it, there might be accidental flipping of the MTJs state resulting in an unwanted write operation (i.e. a read disturbance). Hence, the current through the MTJ (I_{mtj}) should be kept as low as possible. On the other hand due to increasing variations in sub-32 nm CMOS processes along with variation in MTJ resistance, it becomes really challenging to design a read-sensing scheme that achieves low read-disturbance and high yield ($> 5.5\sigma$). Previous works e.g. current sensing schemes [3], [4] suffer from mismatches in the mirroring transistors and hence do not have a very good yield. Furthermore, they typically operate from a high supply voltage due to voltage headroom requirements and hence consume a lot of power. In this work we try to address these issues to design a robust read sensing circuit for resistive memories which would work for yield $> 5.5\sigma$ and reduce power consumption. The robustness to variations is achieved in mainly two ways. Firstly, due to the pseudo-differential nature (comparing data to two references ‘ref1’ and ‘ref0’) of the sensing scheme we get $2\times$ signal margin as compared to a single reference scheme [3]. Secondly, the offset cancellation of the sense-amplifier (SA) makes it more suitable to tolerate variation from the array due

to MTJ resistance variation. Also due to offset cancellation we can use small sized devices for the SA, which results in lower area and less power. Thus the proposed technique benefits from technology scaling. Furthermore, since the sense amplifier has a differential topology it reduces the effect of supply noise and improves common mode rejection.

II. PROPOSED RESISTIVE DIVIDER BASED READ TECHNIQUE

Fig.1 shows the proposed resistive divider based read sensing technique. The basic principle of sensing the MTJ resistance is comparing a resistive divider output voltage V_O (formed by a ‘ref1’ MTJ and data MTJ) to 2 reference voltages V_H and V_L . V_H and V_L are also generated from 2 resistive divider networks using ‘ref1’ and ‘ref0’ cells. $R_{ref,H}$ and $R_{ref,L}$ are reference ‘1’ and ‘0’ devices respectively. R_{mtj} is the data MTJ to be sensed. In phase Φ_1 , the node ‘in1’ is connected to V_O and the node ‘in2’ is connected to V_L . So V_{in1} is close to $V_{dd}/2$ (if we assume the data bit is ‘1’) and V_{in2} is close to $V_{dd}/3$ (assuming $R_H = 2 \times R_L$). In the next phase Φ_{1B} , ‘in1’ is connected to V_H and ‘in2’ is connected to V_O . Hence, V_{in1} is equal to $V_{dd}/2$ and V_{in2} is close to $V_{dd}/2$. Thus the swing at the node ‘in1’ from phase Φ_1 to Φ_{1B} is smaller than the swing at ‘in2’ i.e. $\Delta V_1 < \Delta V_2$. Whereas if data is ‘0’, $\Delta V_1 > \Delta V_2$. The sense margin is defined as $(\Delta V_1 - \Delta V_2)$. An analytical model of this scheme was simulated to analyze the effect of MTJ resistance variation on the sense margin. The μ and μ/σ of the sense margin (SM) is shown in the Fig.1. R_L and R_H are assumed to be $4K\Omega$ and $10K\Omega$ respectively in the simulations, each having 5% variation. It is also assumed that the read current is kept less than $20\mu A$ to keep the read-disturbance rate low. This corresponds to $V_{dd} \approx 20\mu A \times (10 + 10)K\Omega = 400mV$. As seen from the figure, the proposed sensing scheme improves both the nominal signal margin as well as the mean/sigma as compared to an ideal single-ended voltage sensing scheme. This is mostly due to the pseudo-differential nature of the sensing technique which provides $\sim 2\times$ signal margin compared to a single-ended scheme. In addition to that the voltages V_{in1} (and V_{in2}) are generated using the same $R_{ref,H}$ resistor in both the phases Φ_1 and Φ_{1B} , which reduces the effect of its variation of the sense voltage. The proposed resistive-divider technique also burns less power since V_{dd} is smaller ($\sim 400mV$) compared to the nominal V_{cc} ($\sim 1V$, due to voltage headroom requirements) for ideal voltage sensing.

The reference devices can be implemented in the memory array itself and they can be shared by a sub-array (or sector)

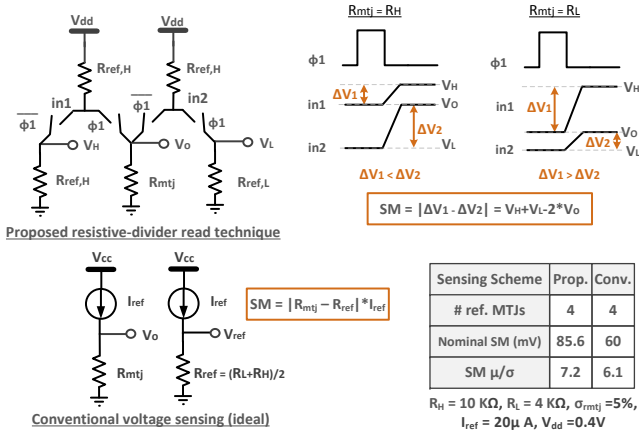


Fig. 1. Proposed resistive-divider read technique for STT-RAM, comparison of simulated sense margin (SM) with a conventional ideal voltage sensing scheme.

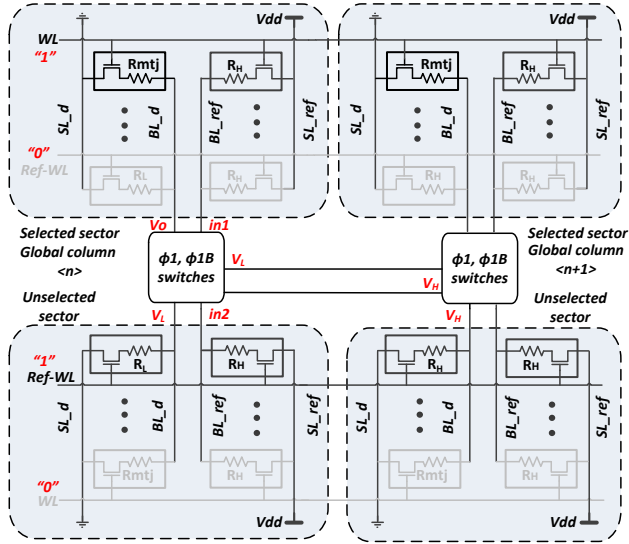


Fig. 2. Array implementation of the reference devices (shown for two global columns), with the reference voltages (V_H , V_L) generated from the unselected sector.

to reduce their area overhead. Fig.2 shows the implementation of the four reference devices. There is one reference row per sector (driven by ‘Ref_WL’) and one reference column per global column (with ‘BL_ref’ and ‘SL_ref’). The reference column and reference row implement the top and bottom devices respectively, of the resistor-divider stack in Fig.1. Since the voltages at the nodes ‘in1’ and ‘in2’ are needed simultaneously, the unselected sector (shown in the bottom part of Fig.2) is used to generate the reference voltages (V_H , V_L) by operating the switches in phases Φ_1 and Φ_{1B} as described in Fig.1. To further reduce the area-overhead of implementing the reference devices, instead of having two separate reference rows the $R_{ref,H}$ and $R_{ref,L}$ devices (in the lower part of the resistor-divider stack) are shared between two adjacent global columns. They generate the reference voltages for the two adjacent global columns in a time-interleaved manner, i.e. the Φ_1 and Φ_{1B} signals for the global column $\langle n \rangle$ are opposite to that of the global column $\langle n+1 \rangle$.

III. PROPOSED SENSE-AMPLIFIER WITH FULL OFFSET-CANCELLATION

The difference of V_O from the 2 reference voltages V_H and V_L are fed as the 2 inputs of a differential sense amplifier. The sense amplifier (SA) consists of 2 inverters which can be reconfigured both as an amplifier and a latch, similar to [5]. We propose a technique to fully cancel the trip-point (V_{trip}) mismatch of the 2 inverters to reduce the sense-amplifier offset voltage.

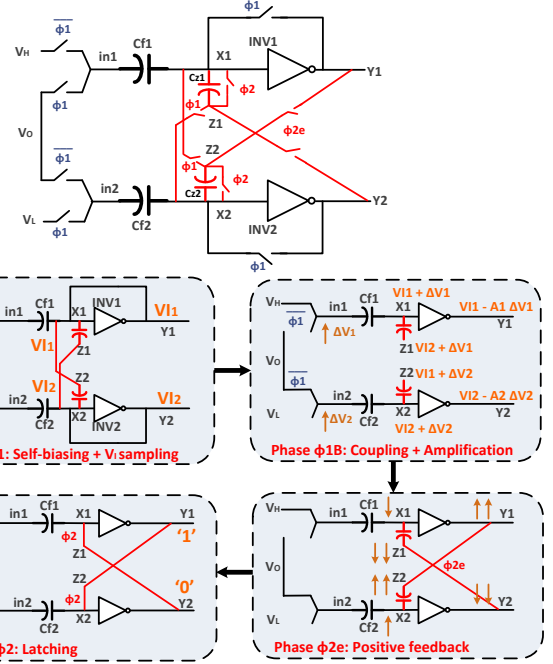


Fig. 3. Proposed sense-amplifier with full offset cancellation of inverter trip point mismatch ($V_{I1} \neq V_{I2}$) by addition of an extra phase (Φ_{2e}) and using extra sampling capacitors (C_{Z1} and C_{Z2}). Shown for the case of $\Delta V_1 < \Delta V_2$, i.e. data ‘1’.

Fig.3 shows the proposed sensing circuit. The nodes ‘in1’ and ‘in2’ are from the resistive divider network described above. During phase Φ_1 , the two inverters ‘inv1’ and ‘inv2’ are biased at their respective trip points. This self-biasing scheme makes sure that the inverters are biased in their high gain (amplifying) region irrespective of device variation. During this phase the sampling capacitors (C_{z1} and C_{z2}) samples the difference of the trip points of the 2 inverters. Next, in phase Φ_{1B} , the negative feedback for the inverters is disconnected. The swing at the nodes ‘in1’ and ‘in2’ are coupled to the input of the inverters via the coupling capacitors (C_{f1} and C_{f2}). The swing at the input of the inverters is amplified by their gain (A) at the outputs (‘y1’ and ‘y2’). The nodes ‘z1’ and ‘z2’ of the capacitors C_{z1} and C_{z2} are floating in this phase, so they do not provide any extra loading at the input of the inverters. After this, in phase Φ_{2e} , ‘z1’ is connected to ‘y2’ and ‘z2’ is connected to ‘y1’. This creates a positive feedback circuit (as long as $C_z > C_f/A$). So the inputs ‘x1’ and ‘x2’ will move in opposite directions (from the respective V_{trip} points), depending on whichever of ΔV_1 and ΔV_2 is higher. Similarly, the outputs ‘y1’ and ‘y2’ will move in opposite directions. It should be noted that even if the trip points of the two inverters are different, it does not affect the positive feedback since the

difference of V_{trip1} and V_{trip2} was already sampled across C_{z1} and C_{z2} during phase Φ_1 . By doing this we can fully cancel the offset due to V_t -mismatch in the 2 inverters. Finally, in phase Φ_2 the capacitors C_{z1} and C_{z2} are shorted, completing the latch. The waveforms of both the SAs are shown in Fig.4 for a case where there is significant mismatch of the V_{trip} of the 2 inverters. As seen from the figure the proposed SA was able to resolve the data correctly due to the full offset cancellation technique.

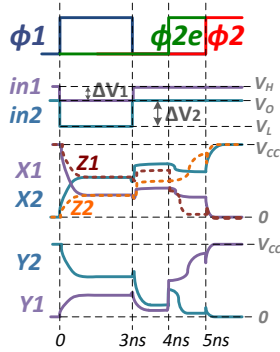


Fig. 4. Simulation waveforms for the conventional and proposed sense amplifiers when there is a mismatch of the V_{trip} of the two inverters. Shown for the case of $\Delta V_1 < \Delta V_2$, i.e. data ‘1’.

Table I shows the effect of variation on the simulated SA offset voltage (V_{off}). The proposed SA provides $\sim 3\times$ improvement in $\sigma(V_{off})$. The low sigma due to offset cancellation suggests that small sized transistors can be used for the sensing inverters and hence the SA power can be reduced. On the other hand, the SA area which is mainly dominated by the size of the sampling capacitors also reduces with CMOS scaling. This is because the capacitors can be implemented by regular MOS transistors. Hence the proposed SA benefits from technology scaling in terms of both area and power metrics, which is very desirable when designing for future resistive memory technologies. Table I also shows the effect of supply noise on σ . For this analysis the V_{cc} of the SA is switched by ΔV_{cc} from phase Φ_1 to Φ_{1B} . This is because changing V_{cc} in phase Φ_{1B} shifts the inverter trip points and this shift did not get sampled during phase Φ_1 . Hence, this step jump in V_{cc} can have a negative impact on the SA operation. However, because the proposed scheme is differential it is more immune to supply noise (which is a common mode signal) than a single-ended sensing scheme [6].

TABLE I. VARIATION ANALYSIS (SIMULATED) AND EFFECT OF SUPPLY NOISE ON THE PROPOSED SA.

| Offset voltage (mV) | Conventional | Proposed |
|--------------------------------|--------------|----------|
| Mean (μ) | 0.2 | 0.1 |
| Standard deviation(σ) | 7.0 | 2.1 |
| $\mu+4\sigma$ | 28.2 | 6.4 |

| % Vcc noise | σ of the proposed SA mV) |
|-------------|---------------------------------|
| 0 | 2.1 |
| 5 | 3.4 |
| 10 | 4.4 |

IV. SILICON IMPLEMENTATION AND MEASUREMENT RESULTS

The proposed SA was implemented in a 14nm CMOS technology. The capacitors in the design (C_f, C_z) are realized using MOSFET devices to limit the technology cost while still achieving a compact footprint of $8\mu m^2$. To facilitate offset characterization, the resistive divider output voltages (V_H, V_L , and V_O) are provided externally through the pads as shown in Fig.5. A Schmitt trigger and a timing control block is integrated on-die to relax the tester requirements. After the DC inputs are set, START is asserted, and the timer generates all the phase clocks that are necessary for SA operation as described in Section III. The SA output becomes available on the D_{out} pin at the end of Φ_2 , and is held by the SA in the latch state until D_{out} value is recorded and START is deasserted for the next measurement.

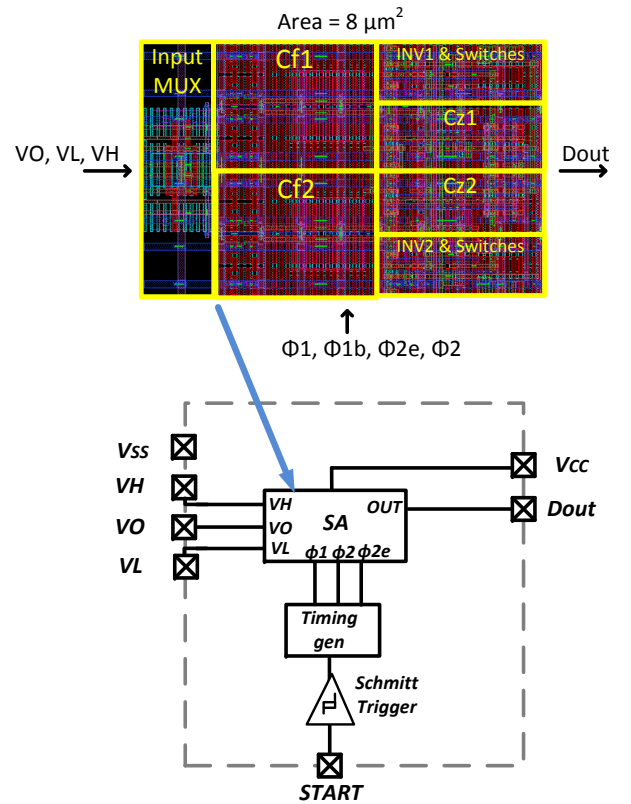


Fig. 5. Sense amplifier layout and test structure including a Schmitt trigger and a timing generator block.

The trip points of 71 SA instances were measured by stepping V_O from V_L (100 mV) to V_H (150 mV) with a 2mV resolution. Each instance was tested 16 times and the V_O levels that can reliably produce ‘0’ or ‘1’ at the output were recorded. Fig.6 shows the distributions of the trip voltage (defined as $V_O - 0.5 \times (V_L + V_H)$) for both low-to-high and high-to-low transitions. The low-to-high trip point varies with a (μ, σ) of (11.3 mV, 2.6 mV) whereas the distribution of the high-to-low trip voltage has a (μ, σ) of (-9.6 mV, 3.2 mV). All the 71 SAs are able to reliably detect input signal levels beyond 20 mV in all 16 runs. We suspect that the data uncertainty within the 20 mV input range is partly caused by random AC noise events in our test environment, since the pre-silicon validation had

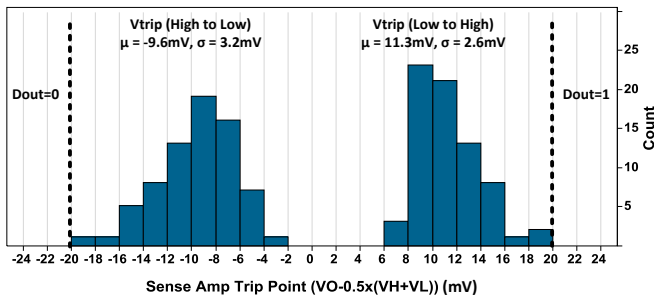


Fig. 6. Measured SA trip point distributions showing the V_O levels that can reliably produce high and low at data out. Collected from 71 SA instances where each instance was tested 16 times.

confirmed the design to have a good tolerance to supply noise and low thermal noise. The AC noise is subtracted from the data by computing the average trip voltage of each SA from the 16 measurements. The DC offset is then defined as twice the difference between the measured average and ideal trip points. Fig.7 shows that the DC offset varies with a standard deviation of 1.9 mV, matching reasonably well to the expected value of 2.1 mV.

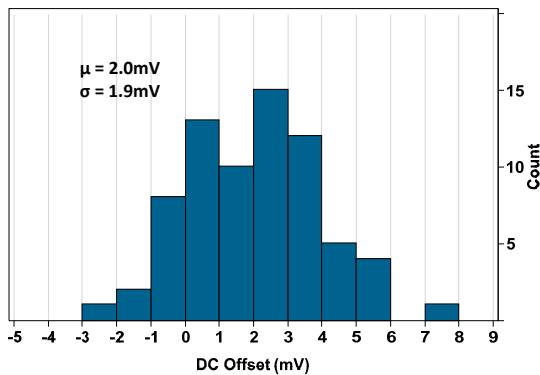


Fig. 7. Measured DC offset from 71 SAs. Each SA was tested 16 times and random noise was removed from data by computing the average trip point. DC offset is then defined as twice the difference between the measured average and ideal trip points.

V. CONCLUSION

In this work we presented a four-phase differential sense amplifier (SA) with an offset cancellation technique for voltage divider based read sensing of resistive memories in a 14nm CMOS process. 71 tested sense amplifiers achieve correct operation with 20mV input and achieve a DC offset σ of 1.9mV. This shows that the SA can tolerate large variations from the memory array to achieve a high yield. On the other hand, due to the offset-cancellation technique the SA can be designed using small sized devices to achieve low area and power.

ACKNOWLEDGMENT

The authors would like to thank Pulkit Jain for his inputs on the sense amplifier design, and others from Intel who supported the layout and silicon testing.

REFERENCES

- [1] Y. Chen and C. Petti, "ReRAM technology evolution for storage class memory application," in *2016 46th European Solid-State Device Research Conference (ESSDERC)*, Sept 2016, pp. 432–435.
- [2] Y. Lu *et al.*, "Fully functional perpendicular STT-MRAM macro embedded in 40 nm logic for energy-efficient IOT applications," in *2015 IEEE International Electron Devices Meeting (IEDM)*, Dec 2015, pp. 26.1.1–26.1.4.
- [3] M. Jefremow, T. Kern, W. Allers, C. Peters, J. Otterstedt, O. Bahlous, K. Hofmann, R. Allinger, S. Kassenetter, and D. Schmitt-Landsiedel, "Time-differential sense amplifier for sub-80mV bitline voltage embedded STT-MRAM in 40nm CMOS," in *2013 IEEE International Solid-State Circuits Conference Digest of Technical Papers*, Feb 2013, pp. 216–217.
- [4] C. Kim, K. Kwon, C. Park, S. Jang, and J. Choi, "A covalent-bonded cross-coupled current-mode sense amplifier for STT-MRAM with 1T1MTJ common source-line structure array," in *2015 IEEE International Solid-State Circuits Conference - (ISSCC) Digest of Technical Papers*, Feb 2015, pp. 1–3.
- [5] B. Giridhar, N. Pinckney, D. Sylvester, and D. Blaauw, "A reconfigurable sense amplifier with auto-zero calibration and pre-amplification in 28nm CMOS," in *2014 IEEE International Solid-State Circuits Conference Digest of Technical Papers (ISSCC)*, Feb 2014, pp. 242–243.
- [6] N. Verma and A. P. Chandrakasan, "A High-Density 45nm SRAM Using Small-Signal Non-Strobed Regenerative Sensing," in *2008 IEEE International Solid-State Circuits Conference - Digest of Technical Papers*, Feb 2008, pp. 380–621.